Journal of Applied Polymer Science

Flame Retarding Effect of Graphite in Rotationally Molded Polyethylene/Graphite Composites

Washington Mhike,[1] Ignatius V. W. Ferreira,[1] Jing Li,[2,3] Stanislav I. Stoliarov,[2,3] Walter W. Focke[1]

[1]Institute for Applied Materials, Department of Chemical Engineering, University of Pretoria, Private Bag X20, Hatfield, Pretoria, 0028, South Africa

[2]Department of Fire Protection Engineering, University of Maryland, College Park, Maryland 20742

[3]Department of Mechanical Engineering, University of Maryland, College Park, Maryland 20742

Correspondence to: W. W. Focke (E-mail: walter.focke@up.ac.za)

ABSTRACT: Linear low-density polyethylene (LLDPE) compounds containing 10 wt % graphite fillers were rotationally molded into flat sheets. Flame retardancy was studied using cone calorimeter tests conducted at a radiative heat flux of 35 kW/m^2. Only the expandable graphite, an established flame retardant for polyethylene, significantly reduced the peak heat release rate. Compared with the neat polyethylene, it was easier to ignite the LLDPE composites containing carbon black, expandable graphite, and exfoliated graphite. However, rather unexpectedly, the inclusion of flake graphite increased the time to ignition by up to 80%. Simulations conducted with the ThermaKin numerical pyrolysis software suggest that increased reflectivity was mainly responsible for this effect.
 J. Appl. Polym. Sci. **2015**, *132*, 41472.

KEYWORDS: flame retardance; polyolefins; properties and characterization

Received 19 June 2014; accepted 2 September 2014
DOI: 10.1002/app.41472

INTRODUCTION

Polyethylene is extensively extruded into pipes and cables, and rotomolded to produce tanks, containers, battery boxes, and ventilation ducting. In underground mining applications such polyethylene-based products pose a severe fire hazard. Flame retardant additives can be added to reduce the fire risk.[1] However, owing to its aliphatic nature, polyethylene presents unique challenges. It melts and drips easily, is noncharring, and has a high heat of combustion.[2] Halogen-based flame retardants are effective but they may release toxic fumes and dense smoke. This is particularly troublesome in underground mining with its confined spaces and limited access to ventilation. Metal hydrate-based flame retardants, e.g., aluminum trihydrate do not present significant toxicological or environmental concerns.[1,3] However, they require high loadings to be effective and this affects mechanical properties negatively.

Recent studies have highlighted the utility of expandable graphite, intumescent flame retardants and their synergistic combinations for improving the fire behavior of polyethylene.[2,4–9] Intumescent additives cause the material to swell when exposed to high heat and form a carbonaceous foam residue that acts both as a heat insulator and a physical barrier to the transport of pyrolysis products.[10–13]

Expandable graphite is made by partial oxidation of the flake graphene sheets with simultaneous intercalation (i.e., insertion) of charge-neutralizing guest species (e.g., sulfuric acid anions) in-between the stacked graphene layers.[14] Upon exposure to high temperatures, the intercalated guest molecules decompose into gaseous species that causes the flakes to expand rapidly in a worm-like manner.[15,16] Expandable graphite is an effective intumescent flame retardant for polyethylene at loading above 10 wt %.[17]

Polyethylene is an insulator material and the high surface resistivity allows the build-up and retention of static charges on product surfaces. Static electricity poses both a nuisance and a hazard as it is a potential ignition source for fires. Flake graphite is a layered sheet mineral that can be added to polyethylene to impart suitable antistatic properties.[18]

Our overall objective is to develop cost-effective flame retarded and antistatic polyethylene compounds with good thermal conductivity suitable for rotomolding. The aim of this particular study was to investigate the flame retarding effect of graphite in rotationally molded polyethylene/graphite composites. Various graphite forms were considered, including flake graphite, expandable graphite, and exfoliated graphite. ThermaKin software was used to help with the interpretation of cone calorimeter fire test results.

EXPERIMENTAL

Materials

The linear low-density polyethylene (LLDPE) was supplied by Sasol Polymers. It was a hexene comonomer-based rotomolding grade powder (Grade HR 411: MFI 3.5 @190°C/2.16 kg); density 0.939 g/cm^3; particle size: 90% < 600 μm). Natural Zimbabwean flake graphite was obtained from BEP Bestobell, Johannesburg. Chemserve Systems supplied the release agent Sliprolease 20 K and Orchem provided the antioxidant Orox PK (polymerized 2,2,4-trimethyl-1,2-dihydroquinoline). Two grades of expandable graphite ES250 B5 (onset temperature 220°C) and ES170 300A (onset temperature 300°C) were obtained from Qingdao Kropfmuehl Graphite (China). The latter constituted the expandable form used in this study. The former could not be used for rotomolding as the expansion onset temperature was too low.

Methods

The exfoliated graphite form was prepared by exposing the ES250 B5 grade powder to high heat for 5 min by placing it in a Thermopower electric furnace set at 600°C. A dry-blend formulation was prepared as follows. The exfoliated ES250 B5 (10 wt %) and the antioxidant Orox PK (2 wt %) were mixed with the LLDPE powder in a high speed mixer-grinder for 5 min. The same blending procedure was used to make a dry-blend containing the ES170 300A graphite. These powder mixtures were used directly to rotomold test samples.

A slightly different procedure was used to prepare the carbon black and flake graphite composites. The filler (10 wt % carbon black or flake graphite) was manually mixed with polyethylene powder. The samples were melt-compounded in a 40-mm corotating Berstorff twin screw extruder using the processing conditions reported by Mhike and Focke.[18] The composite strands were water cooled, air dried and granulated into pellets. These were then milled into rotomolding powder using a Pallmann 300 pulverizer. The antioxidant Orox PK (2 wt %) was blended into the milled powder using a kitchen blender for 1 min.

A stainless steel rectangular cuboid mold with inside dimensions 200 × 150 × 100 mm was used for rotomolding. A constant volume of material (320 cm^3) was used for all compositions to obtain a constant part thickness of ca. 3.0 mm. The charge mass was adjusted by considering the density of the various components. The rotomolding machine was a modified Thermopower convection oven that was fitted with a biaxial mold rotating mechanism. The rotomolding process parameters were previously reported by Mhike and Focke.[18] The mold was cooled in the oven using ambient air.

Characterization

The graphite particle size distributions were determined with a MastersizerHydrosizer 2000 (Malvern Instruments, Malvern, UK). The Brunauer–Emmett–Teller (BET) specific surface areas of the graphite powders were determined with a Nova 1000e BET in N_2 at 77 K. True densities were determined on a Micrometrics AccuPyc II 1340 helium gas pycnometer. The elemental composition of the graphite powders was determined by X-ray fluorescence (XRF) analysis performed using the ARL 9400XP+ XRF spectrometer. The samples were pressed into powder briquettes and introduced to the spectrometer.

The bulk density of 2.7 × 15 × 15 mm pieces of rotomolded sheets was evaluated on a Micrometrics GeoPyc 1360 envelope density analyzer. Five cycles were performed on each sample and the reported values represent averages of three tests.

Thermogravimetric analysis (TGA) of the neat LLDPE was performed on a Mettler-Toledo TGA 850^e machine or a Perkin-Elmer TGA 4000 instrument. Seventy-microliter alumina pans were used to hold the samples. Sample masses of between 4 and 7 mg were heated from 25 to 600°C at 10°C/min under air flow (50 mL/min). The same method was also used for the rotomolded 10 wt % graphite/polyethylene composites prepared by melt compounding except that TGA runs were also performed under nitrogen. The enthalpies of melting and of decomposition of the LLDPE were determined from differential scanning calorimetry (DSC) data. Three samples with mass between 4 and 7 mg of neat LLDPE were analyzed in a Mettler Toledo DSC 1 Star^e System Thermal Analyzer using a heating rate of 10 K/min under air flow (50 mL/min). Closed aluminum pans with pin holes were used to hold the samples.

Polished cross-sections of the molded composites were prepared to study the distribution of the graphite fillers in the composites. Sectioned samples pieces were first cast in an epoxy resin (Specifix 20). After the resin had set, they were polished on a Buehler Alpha 2 speed grinder-polisher. These specimens were viewed with a Zeiss Imager fitted to an A1m optical microscope under the epi-polarized light mode.

The morphology of the composites was also observed using scanning electron microscopy (SEM). Samples were fractured in liquid nitrogen and coated with gold in an Emitech K550 X coating machine. The fracture surfaces were viewed using an acceleration voltage of 5 kV in a JEOL JSM 5800LV machine. The graphite particle morphologies were also studied using this instrument.

Thermal conductivities were determined with a ThermTest Inc. Hot Disk® TPS 500 Thermal Constants Analyzer using the transient plane source method. Measurements were performed on 42 × 42 mm squares cut from the rotomolded sheets. A 6.403 mm Kapton disk type sensor was sandwiched between two sample sheets. A LLDPE disc was inserted in between the sample and the sample holder on both sides of the sample so as to reduce any heat loss. Each result was an average of three tests.

Fire tests were conducted according to the ISO 5660-1 standard on a Dual Cone Calorimeter (Fire Testing Technology (UK) Ltd.). Specimens with lateral dimensions of 100 × 100 mm^2 and an average thickness of 2.70 ± 0.17 mm were wrapped in aluminum foil and exposed horizontally to an external heat flux of 35 kW/m^2. Tests were conducted in triplicate and average results are reported. Additional gasification experiments were conducted under nitrogen using the FTT Controlled Atmosphere attachment to determine whether surface oxidation played a role in the ignition behavior.

Open flame fire tests were conducted on rotomolded sheets that were mounted vertically and exposed to a 40-mm butane flame perpendicular to the sample surface. The times to ignition were

Table I. Mean Particle Size, Surface Area, and Density of the Various Graphite Filler Types

Graphite type	d_{50} (μm)	Surface area (m^2/g)	Density (g/cm^3)
Flake graphite	112	4.0	2.34
Expandable graphite ES250 B5	381	2.4	2.08
Exfoliated graphite ES250 B5	—	16.3	0.66
Expandable graphite ES170 300A	521	2.09	2.23

determined from video camera clips and the burn-through-times from movie clips taken with a Dias Pyroview 380L infrared camera. The latter was placed at a 45° angle to the sample surface at a distance of 200 mm from behind each sample.

RESULTS

Graphite Particle Characteristics

Table I shows the physical properties of the graphite types used in this study. Detailed information on particle size distributions of the various graphite types were previously reported by Mhike and Focke.[18] The d_{50} particle size of the flake graphite (Table I) was about four times lower than that of the two expandable graphite grades. The BET surface areas in Table I show that the surface area of the expandable graphite increased almost sevenfold when it exfoliated on heat treatment at 600°C. SEM micrographs (Figure 1) show the flake-like nature of the flake and expandable graphite samples. The exfoliated graphite, which is shown in Figure 1(C), has a worm-shaped, accordion-like structure. Slit-shaped gaps between the graphite platelets are clearly visible.

XRF results revealed that the carbon content of the flake graphite was about 92 wt %. The main impurities were silica and clay minerals. The organic content of both the two expandable graphite samples were 90 and 88 wt % for ES250 B5 and ES170 300A, respectively.

Thermal Conductivity

Table II reports the thermal conductivities of the polyethylene/graphite composites as measured at ambient conditions. Incorporation of graphite fillers at 10 wt % enhanced the thermal conductivity by at least 33%. However, the highest conductivity found was only 0.68 W m^{-1} K^{-1} for the exfoliated graphite composite. This composite also featured a low electrical resistivity and therefore good antistatic performance.[18] This was attributed to presence of interconnected particle clusters that were observable in both optical and SEM micrographs of the composites.[18] It is known that dispersion states in which graphite particles form conductive chains also results in composites with higher thermal conductivities.[19]

The high porosity observed in the final moldings also explains, in part, the relatively low thermal conductivity values of the composites.[18,20,21] Optical microscopy confirmed the presence of pores in the molding walls.[18] The residual porosity in the

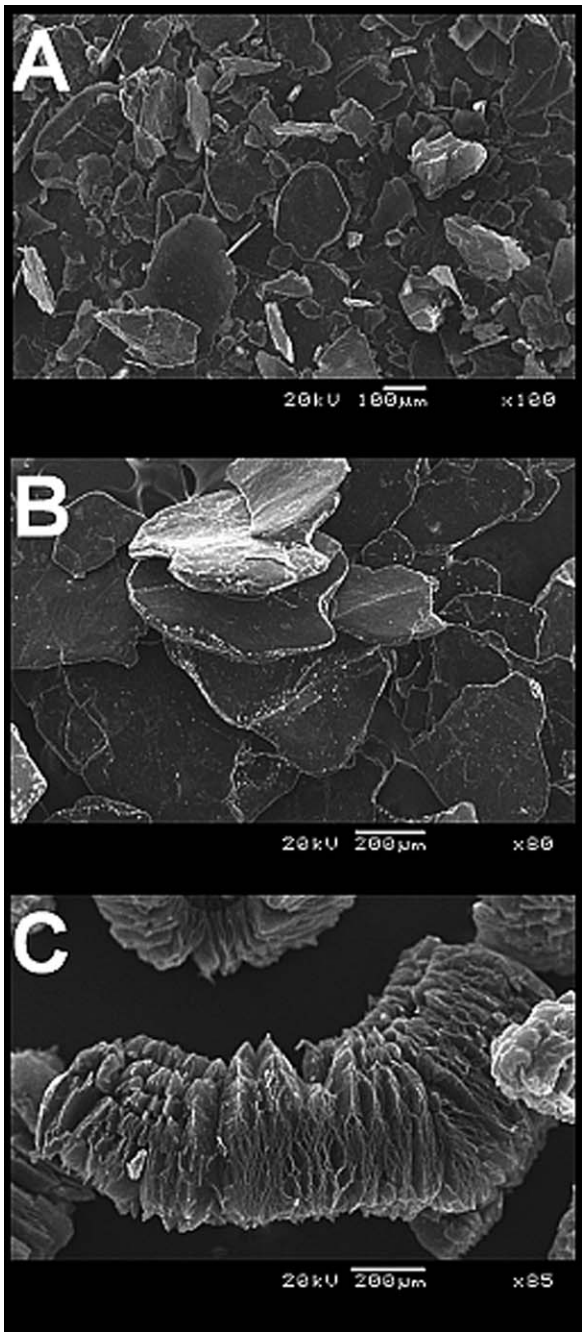

Figure 1. SEM micro graphs of the flaky nature of (A) flake graphite, (B) expandable graphite (ES170), and (C) the 'worm-like structure' of exfoliated graphite (ES250 B5).

Table II. Room Temperature Thermal Conductivity (k) of the Rotomolded Polyethylene/Graphite Composites

Sample	k, W m^{-1} K^{-1}
Neat LLDPE	0.42 ± 0.01
Carbon black	0.38 ± 0.01
Expandable graphite	0.57 ± 0.02
Exfoliated graphite	0.68 ± 0.02
Flake graphite	0.56 ± 0.00

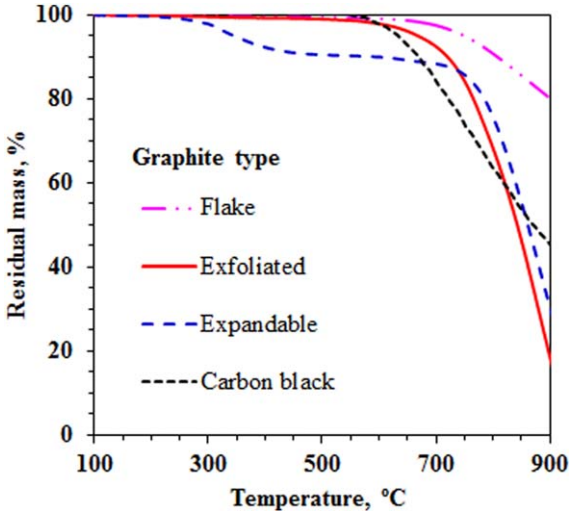

Figure 2. Thermogravimeric analysis curves obtained in air for the graphite fillers. [Color figure can be viewed in the online issue, which is available at wileyonlinelibrary.com.]

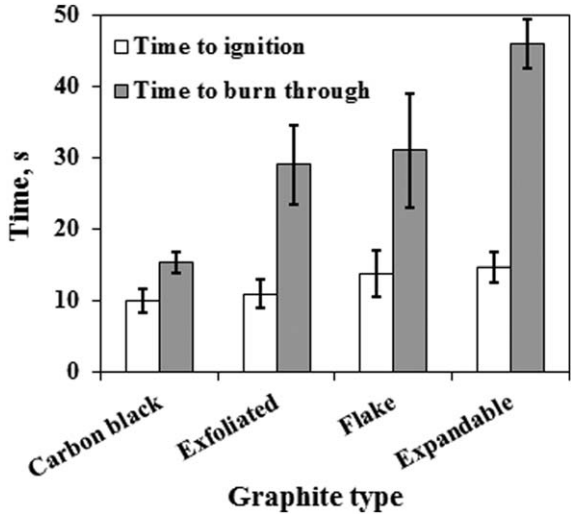

Figure 4. Ignition and burn through times for vertical flame tests. The sample sheets were mounted vertically and exposed to a 40-mm butane flame at perpendicular to the surface.

rotomolded composites was caused by the presence of the flake-shaped graphite particles. They constituted physical barriers to gas transport and increased the effective melt viscosity. Both these effects limit the rate of degassing and thereby prevented the full consolidation of the melt during the rotomolding process.[18]

Thermo Gravimetric Analysis (TGA)

Figure 2 shows thermo gravimetric traces obtained in air for the graphite fillers. The flake graphite and exfoliated graphite only lost weight beyond 600°C. However, the expandable graphite lost about 10% mass between 300 and 500°C owing to the release of gases during the exfoliation. Figure 3 shows thermogravimetric traces in air and in nitrogen for the rotomolded 10 wt % polyethylene/graphite composites. In an air atmosphere the neat polyethylene starts to loose mass just above 400°C and mass loss is virtually complete by 500°C. Surprisingly the carbon black-filled compound was less stable both in air and in nitrogen. Usually one expects carbon black to have little or no effect on the thermo-oxidative degradation of polyolefins.[22–25] However, Hawkins et al.[25] showed that addition of carbon black can adversely affect the performance of phenolic antioxidants commonly added to stabilize polyethylene against thermo-oxidative degradation. They attributed this adverse effect to adsorption of the antioxidant by carbon black. However, this does not explain the slightly higher rate of pyrolysis in nitrogen observed for the carbon black-filled compound. Thus a satisfactory explanation is extant and will require further research.

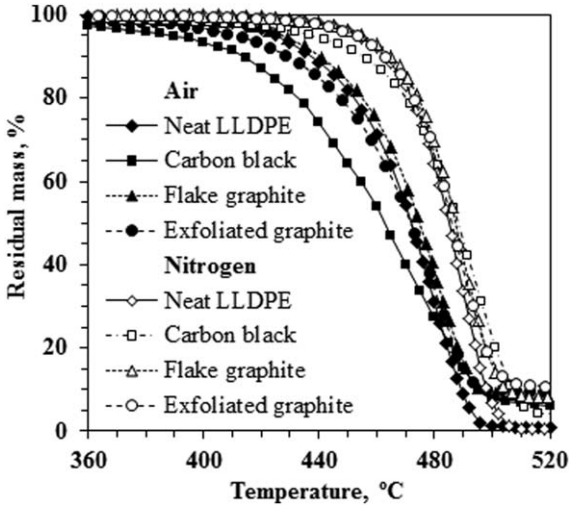

Figure 3. Thermogravimeric analysis curves obtained in air and nitrogen for rotomolded LLDPE and its composites containing 10 wt % graphite fillers.

The flake-shaped fillers particles are thermally stable at the polyethylene pyrolysis temperatures. However, compared with the carbon black composites, they do present a barrier to mass transfer of the pyrolysis products from the condensed phase to the gas phase. This explains the slight shift of the mass loss curves to higher temperatures in the presence of the graphite fillers. It is assumed that the graphite fillers did not otherwise affect the rate of the pyrolysis reactions occurring in the polyethylene matrix. In a nitrogen atmosphere all the samples showed higher thermal stability. Compared at similar mass loss levels, the TGA curves were shifted to higher temperatures by up to 30°C. Furthermore, the mass loss was similar for the three samples shown in Figure 3.

Open Flame Testing

Figure 4 reports the ignition and burn through times recorded for the open flame fire testing of the various samples. Compared with the carbon black pigmented sample, the average ignition times of the flake graphite and expandable graphite compounds were longer. However, the differences cannot be regarded as statistically significant at this point in time owing to the considerable scatter in the data. This is not the case for the burn-through times. Replacing the carbon black with exfoliated graphite or flake graphite doubled the burn-trough time while with the expandable graphite sample it was three times longer.

Table III. Times to Ignition (t_{ig}), Peak Heat Release Rates (*pHRR*), Fire Growth Rates (*FIGRA*), and the Maximum Average Rate of Heat Emission (*MAHRE*) of Polyethylene/Graphite Composites

Composite	t_{ig} (s)	*pHRR* (kW/m^{-2})	*FIGRA* (kW m^{-2} s^{-1})	*MAHRE* (kW/m^2)
Neat LLDPE	82 ± 10[a]	—	—	—
Carbon black	54 ± 14	758 ± 20	5.0 ± 0.2	328 ± 14
Expandable graphite	53 ± 6	360 ± 10	2.9 ± 0.3	217 ± 5
Exfoliated graphite	77 ± 7	793 ± 55	5.0 ± 0.8	292 ± 8
Flake graphite	150 ± 11	725 ± 23	2.7 ± 0.0	191 ± 65

[a] The measured ignition time is suspect as the sample melted and material flowed away.

Cone Calorimeter Fire Testing

Table III and Figure 5 show representative cone calorimeter test results. During the cone calorimeter tests the neat polyethylene melt became fluid and some material flowed away and accumulated underneath the aluminum foil. The mass loss curves showed that about 30% of the material remained at the end of the cone calorimeter tests, i.e. it did not burn away. This means that the cone calorimeter data gathered for the neat polyethylene samples are suspect and, with the exception of the ignition time, they are not reported. Undoubtedly the peak heat release rate and the total heat release were not correctly determined for these samples. Furthermore, the measured (and reported) ignition time is only an upper limit estimate. Removing melt from the heated surface also takes away heat. This retards the generation of flammable vapor and thereby delays the ignition event.

The shape of heat release rate (*HRR*) curves, for thermally thin samples, features a single sharp peak as the whole sample is pyrolyzed almost at once.[26] In contrast the *HRR* curve for a thermally thick, char-producing sample typically shows a rapid rise to a plateau value that is maintained as the sample is progressively consumed.[26] With the exception of the expandable graphite composite, all the heat release curves plotted in Figure 5 exhibited a shape indicative of thermally thin samples.

The *HRR* curve for the expandable graphite composite featured a more flattened shape. It also exhibited the lowest peak heat release rate (*pHRR*) of 360 ± 10 kW/m^2 of all samples tested (Figure 5 and Table III). Both observations can be explained by a protective barrier layer formed at the top surface of the sample by 'worm like' structures resulting from the endothermic expansion of the EG [Figure 1(C)]. This barrier slowed down heat transfer into the substrate during the cone calorimeter testing. The data in Table III also shows that the *pHRR* was basically the same whether the composites contained carbon black, flake graphite or exfoliated graphite as filler. The mean peak heat release rates for these composites, taken together, was 763 ± 43 kW/m^2.

The times to ignition of the carbon black and expandable graphite composites were also statistically indistinguishable and taken together it was 54 ± 10 s. The value for the exfoliated graphite was a little higher (77 ± 7 s). Rather unexpectedly the flake graphite composite featured a significantly longer ignition delay of 150 ± 11 s. This was 80% longer than the value recorded for the neat LLDPE.

Figure 6 compares representative mass loss curves obtained during cone calorimeter testing. Both conventional fire test results obtained in air and gasification results obtained under a nitrogen blanket are presented. In the latter case the samples simply pyrolyzed and there was no flame. The comparison of these two data sets will be discussed in the Discussion section. The slope of such a mass loss curve indicates the mass loss rate (*MLR*). As expected the *MLR* curves (not shown) obtained in the fire tests corresponded well with those of the *HRR* (Figure 5). The expandable graphite composite featured a reduced mass loss rate compared with the other composites. For the flake graphite composite there is also a significant delay before mass loss proceeds in the trace. This parallels the observed delay in the heat release and also accords with the longer ignition time found for this material.

The fire growth rate (*FIGRA*) and the maximum average rate of heat emission (*MARHE*) are indices that may be used to interpret cone calorimeter data.[26,27] The *FIGRA* is an estimator for the fire spread rate and size of the fire whereas the *MARHE* guesstimates the tendency of a fire to develop.[27] The *FIGRA* is defined as the maximum quotient of *HRR*(*t*)/*t*, i.e. the heat

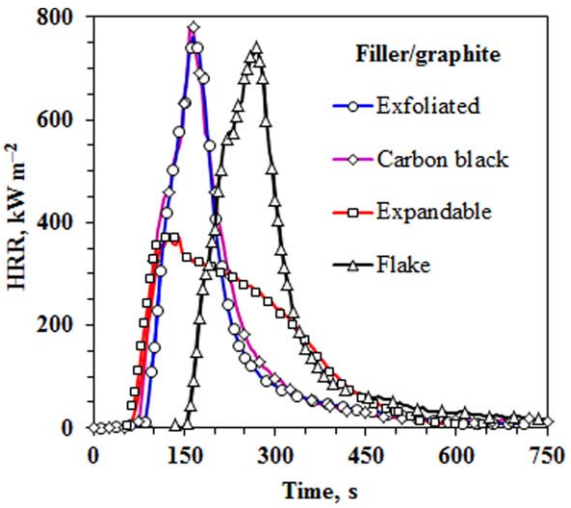

Figure 5. Typical cone calorimeter heat release rate (HRR) curves of rotomolded polyethylene/graphite composites. The sample sheets were backed by aluminum foil and their dimensions were 100 × 100 × 2.7 mm. They were mounted horizontally and exposed from above to an external heat flux of 35 kW/m^2. [Color figure can be viewed in the online issue, which is available at wileyonlinelibrary.com.]

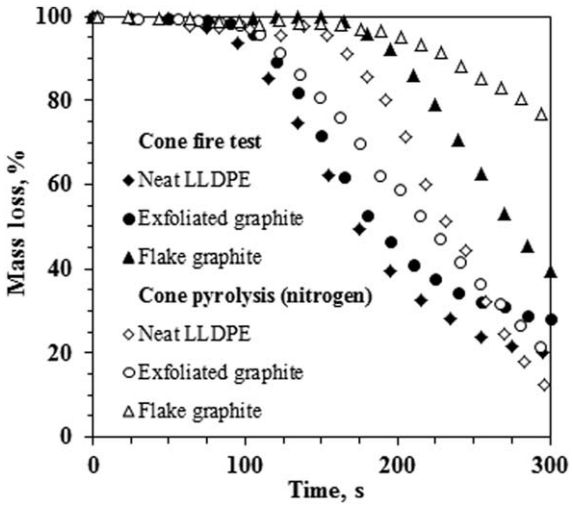

Figure 6. Typical cone calorimeter mass loss curves of rotomolded polyethylene/graphite composites obtained under normal fire test conditions and in a nitrogen atmosphere. The sample sheets were backed by aluminum foil and their dimensions were 100 × 100 × 2.7 mm. They were mounted horizontally and exposed from above to an external heat flux of 35 kW/m^2. Note that the mass loss curves obtained in the cone calorimeter fire tests with the neat polyethylene were limited by the low-viscosity melt flowing away and accumulating below the aluminum film.

release rate up to a time t divided by this time. Usually it can be estimated using the following expression

$$FIGRA = pHRR/time\ to\ pHRR \quad (1)$$

Table III also reports the *FIGRA* and *MARHE* indices. The values of the neat LLDPE could not be determined as it dripped and the melt flowed away during the cone calorimeter tests. The *FIGRA* was expected to be higher as it contained more fuel than the filled compounds. The graphite fillers are stable to high temperatures and therefore reduce the effective solid fuel content. Compared with the carbon black and exfoliated graphite composites, the flake graphite and expandable graphite composites exhibited the lowest *FIGRA* and *MARHE* values. The flake graphite composite had the lowest *MARHE* of 222 kW/m^2. This suggests that it had the lowest propensity of developing into a fire.

Both the *FIGRA* and *MARHE* indices are attempts to capture cone calorimeter performance with a single quantifiable parameter. However, this naïve approach can lead to erroneous conclusions.[26] It would certainly be better to consider the two most important parameters pertinent to fire hazards, i.e. the fire load and flame spread, simultaneously.[26] The fire load is the total amount of heat that can be produced by a flammable material once it is ignited. In the cone calorimeter this index is quantified by the total heat released (*tHR*) during the cone calorimeter test.

Unfortunately the flame spread rate is not directly determined in a cone calorimeter. Petrella[28] proposed the fire growth index ($pHRR/t_{ig}$) as an estimator of the flame spread instead of the *FIGRA*. The Petrella plot helps to visualize the effect of a flame retardant on the magnitude of both fire hazard parameters.[26,28] It is a plot of the total heat released *tHR* (as the fire load) against $pHRR/t_{ig}$ (as a fire growth index). For a material to be effectively flame retarded both the fire load and the fire growth index should assume low values. According to the Petrella plot of Figure 7, the flake graphite composite gave a slightly higher fire load in the present cone tests compared with the other samples while the carbon black composite exhibited the highest fire growth index. The flake graphite composites exhibited the lowest fire growth index mainly because of a longer time to ignition. In contrast, for the expandable graphite composite the reduction of this parameter was mainly due to a reduction in the *pHRR*. To see this, please refer to eq. (1) and Figure 5.

ThermaKin Modeling Results

Numerical simulations with ThermaKin were performed to gain insight into the physical mechanisms responsible for the surprisingly large differences in the ignition times. ThermaKin is a numerical pyrolysis model that can predict the mass loss rate of a solid fuel exposed to a uniform heat flux.[29] ThermaKin solves the mass and energy balances through conservation equations and computes the rate at which the gaseous fuel is produced, with the physical and chemical properties of the solid polymer as the input parameters. ThermaKin has been validated and successfully predicted the results of cone calorimeter tests.[29–32]

The physical properties of the polyethylene polymer are changed by the addition of the flame retardant additives. Beyond this, some properties are also modified by the processing procedure used to prepare the samples. For example, graphite has a higher density than polyethylene so that one would expect the density of the material to increase when it is incorporated. However, in the rotomolding process the presence of these flake-like fillers hampers devolatilization. Because full consolidation is not achieved, the final product density can be lower than that of the polyethylene base.

Several previous studies considered the effect of material physical property variations of cone calorimeter performance parameters.[30,31,33–35] Linteris[36] and Patel et al.[35] used ThermaKin modeling and found that the ignition time increased with increases in density, thermal conductivity, heat capacity, surface reflectivity while it decreased with increase in the absorption coefficient for infrared radiation.

Because the primary concern here is with the times to ignition, the Arrhenius parameters were adjusted to get good fit with the ignition time and approximate shape of the HRR curve for the neat polyethylene. Details of the present simulations are presented in the Appendix. A limitation of the present simulation is that the temperature dependence of physical properties, such as density and thermal conductivity, were not taken into account. However, changes caused by the burning off of the polymer matrix were modeled. The simulations were limited to the carbon black and the flake graphite composites because the objective was to understand why the use of the latter provided longer ignition times. The ThermaKin parameters used in the present simulations are listed in Table IV. Figure 8 shows the predicted heat release rate curves. Their shape differs from those found experimentally (See Figure 5) but the ignition times follow similar trends.

Table IV. Parameters Used in the ThermaKin Simulations

Property	Insulation	LLDPE solid	LLDPE melt	Graphite	Carbon black	Graphite composite	Carbon black composite
K (W m^{-1} K^{-1})	0.11	0.38	0.38	30.82	30.82	0.65	0.42
β (-)	—	—	—	—	—	0.185	0.0168
Cp (at 298 K) (J kg^{-1} K^{-1})	1140	1550	370	700	700	1465	1465
ρ (kg/m^3)	160	939	939	558	545	876	879
Reflectivity (*r*)	0	0.08	0.08	0.3	0.05	0.3	0.05
Absorption coefficient (α) (m^2/kg)	1000	1.1	1.1	8	8	8	8
E (kJ/mol)	—	—	280	—	—	280	280
k_o (s^{-1})	—	—	5.47×10^{22}	—	—	5.47×10^{22}	5.47×10^{22}
Heat of melting (kJ/kg)	—	193	—	—	—	193	193
Heat of decomposition (kJ/kg)	—	920	920	—	—	920	920
Melting temperature (K)	—	378		—	—		
Decomposition temperature (K)	—	678		—	—	678	678

In the ThermaKin simulations the time to ignition was taken as the time at which the *HRR* exceeded 10 kW/m^2.[30] Considering the neat LLDPE, ThermaKin predicted it's time to ignition (t_{ig}) to be 75 s. In comparison with the experimental values of 82 s, ThermaKin under predicted the t_{ig} by 8.5%. The ThermaKin predicted t_{ig} values for the flake graphite-LLDPE and carbon black composites were 99 and 62 s, respectively (Figure 8). These values are only in fair agreement with the experimentally observed t_{ig} values of 150 and 54 (Table III).

Every important fire index *f* depends on a wide range of material properties and structural variables. This functional relationship can be expressed as

$$f = f(\rho,\ k, Cp, r, \ldots) \tag{2}$$

where the fire index is a member of the set $f \in \{pHRR, MAHRE, FIGRA, t_{ig}, \ldots\}$. Each of these usually depend, in a highly a nonlinear fashion, on the physical properties of the test sample, e.g. density (ρ), thermal conductivity (*k*), heat capacity (*Cp*,), reflectivity (*r*), etc. For instance, when graphite is added to the polyethylene most if not all of these properties will change. The advantage of modeling software such as ThermaKin is that it allows one to study the variation of a fire index when only one property value is changed at a time while keeping all the others constant.[31] This was previously performed in a general way by Linteris.[36] The power of such analyses lies in the fact that it can provide clues for the design of flame retardant systems with better performance. The sensitivity of a given fire index *f* to a particular property x_i can be expressed by the relative condition number $C_{R:}$[37]

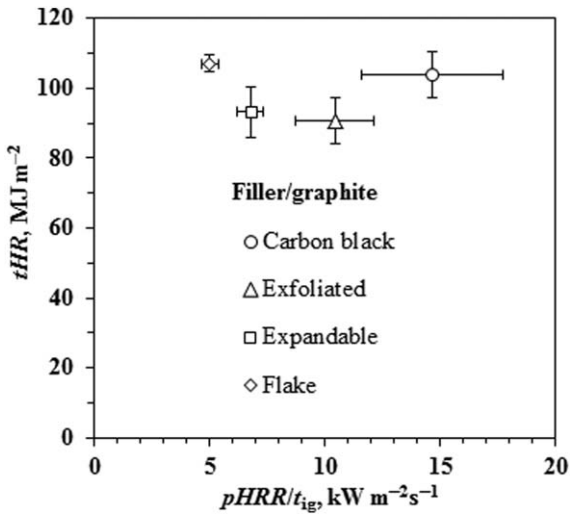

Figure 7. Petrella plot for rotomolded polyethylene/graphite composites.

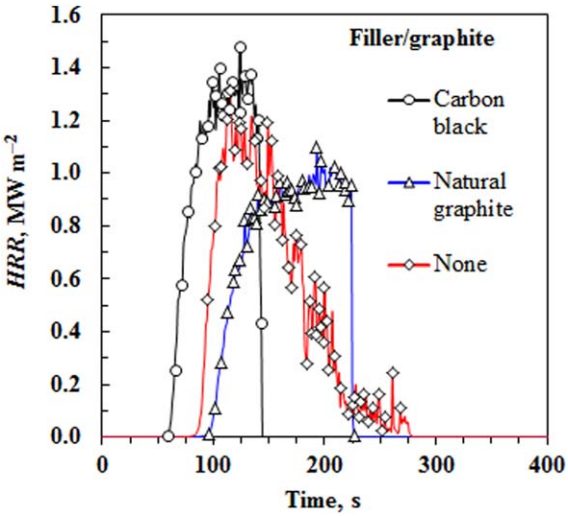

Figure 8. ThermaKin model predictions for the heat release rate (*HRR*) of pure LLDPE and flake graphite-LLDPE and carbon black-LLDPE composites. [Color figure can be viewed in the online issue, which is available at wileyonlinelibrary.com.]

Table V. Effect of Individual Property Value Changes on the Time to Ignition (t_{ig}) and the Apparent Condition Numbers Predicted by ThermaKin Simulations with Neat Polyethylene as Reference

Filler	Property	Units	Property change (%)	Change in t_{ig},(%)	C_R
	Density, ρ	Kg/m^3	−6.7	−13.1	1.94
Graphite	Heat capacity, C_p	J kg^{-1} K^{-1}	−5.5	−9.5	1.74
	Thermal conductivity, k	W m^{-1} K^{-1}	71.1	7.1	0.10
	Reflectivity, r	–	275	47.6	0.17
	Absorption coefficient, α	m^2/kg	6.9	−16.7	−0.03
	Density, ρ	Kg/m^3	−6.4	−16.7	2.61
Carbon black	Heat capacity, C_p	J kg^{-1} K^{-1}	−5.5	−13.1	2.39
	Thermal conductivity, k	W m^{-1} K^{-1}	10.5	6.0	0.57
	Reflectivity, r	—	−37.5	−14.3	0.38
	Absorption coefficient, α	m^2/kg	627	−16.7	−0.03

The indicated property changes reflect those measured for compounds containing either 10 wt % carbon black or 10 wt % flake graphite.

$$C_R(x_i) = \frac{x_i}{f}\left(\frac{\partial f}{\partial x_i}\right) \quad (3)$$

The relative condition number quantifies the sensitivity of a function with respect to small changes in the parameter value x_i. It is clear that the condition number actually depends on the values assumed by the index f and all the physical properties on which f depends and for which it is evaluated. The condition number has a simple interpretation if the effect of a property value on the fire index f can be expressed as a power law function, i.e. $f(x_i) = Kx_i^n$ with K being a constant when all the other property values are fixed. In this case $C_R(x_i) = n$, i.e. it is simply the power law exponent.

Introducing a discrete approximation transforms eq. (3) into

$$\Delta f/f_0 \approx C_R \Delta x_i/x_{i,0} \quad (4)$$

Equation (2) states that the relative change in the fire index f (i.e., $\Delta f/f_o$) is approximately proportional to the relative change in the physical property x_i (i.e., $\Delta x_i/x_{i,o}$) and that the proportionality constant is given by the relative condition number for the property x_i, i.e. $C_R(x_i)$. A large change in the fire index can therefore be expected if both C_R and $\Delta x_i/x_i$ are large. However, even when $C_R(x_i)$ is large, the relative effect on the fire index may nevertheless be small if there is only a small relative change in the physical property x_i.

The C_R values for the time to ignition were estimated using ThermaKin simulations. The neat polyethylene was used as reference state. The effect of the individual property changes introduced by adding either the carbon black or the graphite flakes on the time to ignition were evaluated one by one. The results are presented in Table V. It lists the effect of individual property value changes on the time to ignition (t_{ig}) and the apparent condition numbers predicted by ThermaKin simulations using the neat polyethylene as reference. The indicated property changes reflect those measured for compounds containing either 10 wt % carbon black or 10 wt % flake graphite. The condition numbers calculated using the carbon black and graphite compound properties differ because of the highly non-linear dependence of the time to ignition on sample physical properties. However, the fact that the property changes were different and even rather large in some cases also played a part.

Perusal of the data in Table V indicates that the condition numbers for the sample density and heat capacity are larger than those for the thermal conductivity and reflectivity. However, the addition of these fillers had only a slight effect on the former property values so that the net effect on the time to ignition was marginal. The condition number for reflectivity was relatively small (<0.4) but changing from neat polyethylene to the graphite compound resulted in a large change (almost 50%) in the time to ignition. It is concluded that the ThermaKin simulation results suggest that the longer time to ignition found for the polyethylene graphite composite can be attributed to the high reflectivity of the sample in the presence of the graphite flakes.

DISCUSSION

The flame retardant performance of expandable graphite in polyethylene is actually well known.[4,38,39] The new and surprise finding was that addition of ordinary flake graphite can increase the time to ignition substantially. The sensitivity analysis of the ThermaKin modeling exercise suggested that this was due to the high reflectivity of the flake graphite composite. However, the fact that aliphatic polymers tend to undergo rapid surface oxidation upon heating may offer an alternative explanation.[40] Such oxidation increases the overall rate of formation of gaseous fuel in cone calorimetry-like scenarios and shifts ignition to earlier times. This was previously observed for polypropylene.[40] Its mass loss in nitrogen starts much later than its mass loss in 21% of O_2 (in cone calorimetry like experiments). The present TGA results in air and nitrogen, shown in Figure 3, indicate that the same could be true for polyethylene.

So a possible alternative explanation is that, during pre-ignition heating in the cone, the polymer matrix initially gasifies through oxidation. As the matrix recedes, the graphite (or carbon black) stays behind and forms a thin layer on the surface. The layer formed by the flake graphite happens to be more

effective in blocking environmental oxygen from reaching the rest of polyethylene matrix (perhaps, because the flake graphite itself is most oxidatively stable).

Subjecting a sample with flake graphite and a sample with nano-sized exfoliated graphite to gasification in nitrogen (an experiment that is just like cone calorimetry minus oxygen and flame), should help to determine which mechanism is responsible for the differences in the time to ignition. If the reflectivity hypothesis is correct, the time to onset of mass loss (an equivalent of the time to ignition) for the flake graphite sample will be notably longer than that of nano-sized graphite. If on the other hand the oxygen blockage hypothesis is correct, the time to onset of mass loss will be about the same for both materials and close to the cone result for the flake graphite samples.

The ThermaKin model slightly underpredicts the time to mass loss for gasification in nitrogen. At the same time, for cone calorimetry tests, especially at low radiant heat fluxes, it gives highly overestimated predictions. The fundamental reason for this discrepancy is the same – the model does not account for the role of oxygen in the ignition process. Once flame is established, the oxygen near the surface is consumed and the material pyrolyzes in essentially anaerobic fashion. Therefore, the rest of the modeling predictions are more or less consistent with the experiments.

To test the alternative explanation, gasification tests in nitrogen were conducted in a cone calorimeter operating at a radiant heat flux of 35 kW/m^2. Figure 6 compares this pyrolysis mass loss rate data to those obtained in the ordinary cone fire tests. The time to onset of mass loss, corresponds with a reasonable degree of accuracy, to the time to ignition. The mass loss times were estimated as 170, 100, and 250 s for the neat LLDPE, expandable graphite and flake graphite samples, respectively. The uncertainty in these values is at least $\pm$25 s as the data were noisy and had to be averaged and smoothed heavily. Flake graphite samples still exhibited the longest time to mass loss indicating that the ThermaKin explanation of the mechanism of action, i.e. a high surface reflectivity imparted by this additive, is probably correct. The reduction in the time to ignition due to addition of expandable graphite sample is most likely a result of suppression of in-depth radiative heat transfer, which is significant in neat polyethylene. Note that all the predicted times are a good deal larger those obtained in the cone fire tests, which were obtained at the same radiant heat flux. This discrepancy is indicative of the impact of oxidation reactions at the material surface on the ignition process.

Finally, it is worth mentioning that Schartel et al.[41] have already exploited the idea of increasing the ignition times by reducing the surface absorptivity. They achieved this by depositing thin IR-mirror coatings on the surface of test specimens. Their novel and innovative flame retardancy approach not only increased ignition times by an order of magnitude but also reduced the flame spread and fire growth indices to as little as one-tenth of the values of the uncoated polymers.

CONCLUSIONS

The inclusion of different graphite forms in LLDPE at 10 wt % graphite loading enhanced the thermal conductivity by at least 33% for all the composites.

The peak heat release rates of the flake graphite composites were comparable to those of LLDPE containing carbon black. This is in contrast to the performance of the established intumescent flame retardant, expandable graphite, which significantly reduced the peak heat release rate. However, flake graphite enhanced the ignition resistance of LLDPE by more than 80%.

The fire spread rate and size of the fire as measured by the fire growth rate (*FIGRA*) index and propensity of a fire to develop as measured by the *MARHE* index decreased on inclusion of flake and expandable graphite in the polyethylene matrix. The Petrella plot, which is a measure of the flame retarding effect in the composites encompassing the fire load (total heat evolved) and fire growth index, shows that flake graphite imparts flame retardant properties to LLDPE, particularly for rotomolded composites prepared by dry blending. However, because this is based primarily on a reflectivity increase, flake graphite should only be considered as a component of a more complex flame retardant system for real applications.

ThermaKin modeling results led to the important conclusion that the reflectivity of the composites, especially that of the flake graphite-LLDPE, composite is responsible for the significant differences in the observed times to ignition.

ACKNOWLEDGMENTS

This work is based on research funded by the South African Research Chairs Initiative of the Department of Science and Technology (DST) and the National Research Foundation (NRF) and Xyris Technology CC. Any opinion, findings, and conclusions or recommendations expressed in this material are those of the authors and therefore the NRF and DST do not accept any liability with regard thereto.

APPENDIX: THERMAKIN SIMULATION DETAILS

ThermaKin was used to model the cone calorimeter results for the carbon black and the flake graphite composites. It was assumed that only the LLDPE decomposed while the carbon black and flake graphite remained intact, i.e. they did not undergo any reactions during the cone calorimeter burn tests.

The melting of the LLDPE was treated as a pseudo reaction in the modeling. The LLDPE decomposition reaction was assumed to follow first order kinetics with Arrhenius temperature dependence. The two unknown parameters, namely the pre-exponential constant,k_0 and the activation energy, E were initially estimated from TGA data obtained in nitrogen using the procedure described by Lyon et al.[42] Then the activation energy value was adjusted to get a good fit for the time to ignition for the neat LLDPE measured in the cone calorimeter while the pre-exponential factor was adjusted to get a reasonable fit of the shape of the corresponding *HRR* curve.

It was assumed that neither the heat of melting nor the decomposition of the LLDPE phase was affected by the presence of carbon black or flake graphite. This is justified by the chemical inertness of the fillers and their high thermal stability in the temperature range where the LLDPE undergoes pyrolysis.

Heat capacities were assumed temperature independent and for the composite materials they were estimated using the expression

$$C_p = \sum_{i=1}^{n} C_{p,i} w_i \quad (5)$$

where w_i is the mass fraction of the relevant material component of the composite and $C_{p,i}$ the heat capacity of that component, C_p is the composite heat capacity.

The thermal conductivities of the composites were estimated from

$$k_p = \sum_{i=1}^{n} k_i v_i \quad (6)$$

$$k_n = \left(\sum_{i=1}^{n} v_i / k_i\right)^{-1} \quad (7)$$

$$k = \beta k_p + (1-\beta) k_n \quad (8)$$

where k is the composite conductivity and k_p and k_n are given by eqs. (6) and (7), respectively. In these equations k_i is the thermal conductivity of component i and v_i is volume fraction of that component. The value of β was adjusted so that the thermal conductivities of the composites corresponded to the experimental values listed in Table IV.

It was assumed that the thermal conductivity of the neat polymer melt is the same for that of the neat solid polymer and that the thermal conductivities are temperature independent. The densities of the composites were modeled to match those given in Table IV by manipulating the densities of the graphite and carbon black using eq. (9):

$$\rho_c = \left(\sum_{i=1}^{n} x w_i / \rho_i\right)^{-1} \quad (9)$$

where w_i is the mass fraction of the relevant material and ρ_i the density. The densities of the solid polymer and that of the polymer melt were assumed equal and temperature independent.

Before ignition, the radiative heating is accompanied by convective cooling defined by a convection coefficient. The cooling coefficient was taken as 8.2 W m^{-2} K^{-1} based on the natural convection for a horizontal plate in air [43] with the temperature of the environment as 298 K. In the ThermaKin simulations the convective cooling was set to zero and a radiative flux from the flame was added once ignition occurred. The ignition point is governed by a critical ignition mass flux given as the critical HRR divided by the heat of combustion. The critical HRR for LLDPE was taken as 10 kW/m^2 and the heat of combustion as 40.3 MJ/kg.[30,44] This resulted in an ignition mass flux of 2.48 kg m^{-2} s^{-1}. The radiative heat flux from the flame was taken as 11 kW/m^2, which is the same as that for HDPE.[30] This is believed to be a reasonable assumption as the composition of LLDPE and HDPE are similar. The mass transfer of the gas out of the condensed phase is governed by the gas transfer coefficient. In this case, it was modeled as if the gas had no trouble leaving the condensed phase i.e. it was set sufficiently high as to not have an effect on the HRR. The value of this parameter was set equal to 10^{-5} m^2 s^{-1}.[30]

The sample thickness was set at 2.7 mm and the insulation at the bottom of thickness at 0.025 m. The properties for the insulation (Fiberfrax Durablanket S ceramic blanket) were obtained from the supplier (Yorkshire Refractory Products Limited), with the exception of the emissivity and the absorption coefficient in which it was modeled that all radiation is absorbed. A summary of all the properties, excluding the reflection and absorption coefficient of the composites, used in the modeling is given in Table IV.

REFERENCES

1. Laoutid, F.; Bonnaud, L.; Alexandre, M.; Lopez-Cuesta, J. M.; Dubois, P. *Mater. Sci. Eng. R: Rep.* **2009**, *63*, 100.
2. Weil, E. D.; Levchik, S. V. *J. Fire Sci.* **2008**, 26, 5.
3. Hull, T. R.; Witkowski, A.; Hollingbery, L. *Polym. Degrad. Stabil.* **2011**, *96*, 1462.
4. Qu, B.; Xie, R. *Polym. Int.* **2003**, *52*, 1415.
5. Xie, R.; Qu, B. *J. Appl. Polym. Sci.* **2001**, *80*, 1181.
6. Xie, R.; Qu, B. *J. Appl. Polym. Sci.* **2001**, *80*, 1190.
7. Pang, X. Y.; Song, M. *Adv. Mater. Res.* **2012**, *560*, 779.
8. Sun, Z.; Ma, Y.; Xu, Y.; Chen, X.; Chen, M.; Yu, J.; Hu, S.; Zhang, Z. *Polym. Eng. Sci.* **2014**, *54*, 1162.
9. Han, Z.; Dong, L.; Li, Y.; Zhao, H. *J. Fire Sci.* **2007**, *25*, 79.
10. Camino, G.; Costa, L.; Martinasso, G. *Polym. Degrad. Stabil.* **1989**, *23*, 359.
11. Wang, J. Q.; Chow, W. K. *J. Appl. Polym. Sci.* **2005**, *97*, 366.
12. Lewin, M. *J. Fire Sci.* **1999**, *17*, 3.
13. Dasari, A.; Yu, Z. Z.; Cai, G. P.; Mai, Y. W. *Prog. Polym. Sci.* **2013**, *38*, 1357.
14. Chen, G.; Weng, W.; Wu, D.; Wu, C. *Eur. Polym. J.* **2003**, *39*, 2329.
15. Chung, D. *J. Mater. Sci.* **2002**, *37*, 1475.
16. Wissler, M. *J. Power Sources* **2006**, *156*, 142.
17. Xie, R.; Qu, B. *Polym. Degrad. Stabil.* **2001**, *71*, 375.
18. Mhike, W.; Focke, W. W. *J. Vinyl Addit. Techn.* **2013**, *19*, 258.
19. Agari, Y.; Ueda, A.; Nagai, S. *J. Appl. Polym. Sci.* **1991**, *42*, 1665.
20. Osman, A. F.; Johar, B.; Adam, S. N. F. S.; Amin, S. A. M.; Osman, A. *International Conference on Sustainable Materials Engineering (ICoSM* 2007*)*, Penang, Malaysia, **2007**.
21. Sumirat, I.; Ando, Y.; Shimamura, S. *J. Porous Mat.* **2006**, *13*, 439.
22. Goldberg, V. M.; Kolesnikova, N. N.; Paverman, N. G.; Kavun, S. M.; Stott, P. E.; Gelbin, M. E. *Polym. Degrad. Stabil.* **2001**, *74*, 371.
23. Gilroy, H. M.; Chan, M. G. *Polym. Sci. Technol.* **1984**, *26*, 273.
24. Peña, J. M.; Allen, N. S.; Edge, M.; Liauw, C. M.; Valange, B. *Polym. Degrad. Stabil.* **2001**, *72*, 163.
25. Hawkins, W. L.; Hansen, R. H.; Matreyek, W.; Winslow, F. H. *J. Appl. Polym. Sci.* **1959**, *1*, 37.
26. Schartel, B.; Hull, T. R. *Fire Mater.* **2007**, *31*, 327.
27. Sacristán, M.; Hull, T. R.; Stec, A. A.; Ronda, J. C.; Galià, M.; Cádiz, V. *Polym. Degrad. Stabil.* **2010**, *95*, 1269.
28. Petrella, R. V. *J. Fire Sci.* **1994**, *12*, 14.
29. Stoliarov, S.; Lyon, R. *DOT/FAA/AR-TN08/17* **2008**.
30. Stoliarov, S. I.; Crowley, S.; Lyon, R. E.; Linteris, G. T. *Combust. Flame* **2009**, *156*, 1068.
31. Stoliarov, S. I.; Safronava, N.; Lyon, R. E. *Fire Mater.* **2009**, *33*, 257.

32. Stoliarov, S. I.; Crowley, S.; Walters, R. N.; Lyon, R. E. *Combust. Flame* **2010**, *157*, 2024.

33. Linteris, G.; Zammarano, M.; Wilthan, B.; Hanssen, L. *Fire Mater.* **2012**, *36*, 537.

34. Lyon, R. E.; Safronava, N.; Quintiere, J. G.; Stoliarov, S. I.; Walters, R. N.; Crowley, S. *Fire Mater.* **2014**, *38*, 264.

35. Patel, P.; Hull, T. R.; Stec, A. A.; Lyon, R. E. *Polym. Adv. Technol.* **2011**, *22*, 1100.

36. Linteris, G. T. *Fire Mater.* **2011**, *35*, 463.

37. Higham, N. J. Accuracy and stability of numerical algorithms; Society for Industrial and Applied Mathematics: Philadelphia, PA, USA, **2002**.

38. Kuan, C. F.; Tsai, K. C.; Chen, C. H.; Kuan, H. C.; Liu, T. Y.; Chiang, C. L. *Polym. Composite.* **2012**, *33*, 872.

39. Pang, X. Y.; Duan, M. W.; Tian, Y.; Zhai, M. *Asian J. Chem.* **2013**, *25*, 5390.

40. Fina, A.; Camino, G. *Polym. Adv. Technol.* **2011**, *22*, 1147.

41. Schartel, B.; Beck, U.; Bahr, H.; Hertwig, A.; Knoll, U.; Weise, M. *Fire Mater.* **2012**, *36*, 671.

42. Lyon, R.; Walters, R.; Stoliarov, S. *J. ASTM Int.* **2006**, *3*, 1.

43. Holman, J. P. Heat Transfer; McGraw-Hill: New York, 1986.

44. Lyon, R. E.; Janssens, M. L.; Flammability. Encyclopedia of Polymer Science and Technology. John Wiley & Sons, Inc. **2005**.